# Challenges in Molecular Dynamics of Amorphous ZIFs Using Reactive Force Fields

Nicolas Castel and François-Xavier Coudert*

Read Online

ACCESS | Metrics & More | Article Recommendations | Supporting Information

**ABSTRACT:** While amorphous metal−organic frameworks form an emerging class of materials of growing interest, their structural characterization remains experimentally and computationally challenging. Out of the many molecular simulation methods that exist to model these disordered materials, one strategy consists in simulating the phase transition from a crystalline MOF to the amorphous state using molecular dynamics. ReaxFF reactive force fields have been proposed for this purpose in several studies to generate models of zeolitic imidazolate framework glasses by melt quenching. In this work, we investigate the accuracy and reliability of this approach by reproducing the published procedures and comparing the structure of the resulting glasses to other data, including ab initio modeling, in detail. We find that the in silico melt-quench procedure is extremely sensitive to the choice of methodology and parameters and suggest adaptations to improve the scheme. We also show that the glass models generated with ReaxFF are markedly different from their ab initio counterparts, as well as known experimental characteristics, and feature an unphysical description of the local coordination environment, which in turn affects the medium-range and bulk properties.
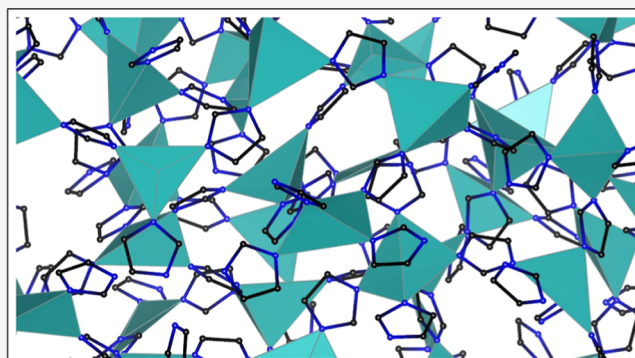


## INTRODUCTION

Metal−organic frameworks (MOFs) are hybrid materials composed of inorganic nodes (clusters or metal ions) bridged by organic linkers to form three-dimensional architectures, often porous. They have been the subject of an intensive research effort for over 20 years and, taking advantage of their porosity and structural and chemical tunability, have been proposed for applications in various industrial-scale processes, such as gas storage and separation or catalysis.[1] The majority of studies in the literature are focused on perfectly ordered, crystalline MOFs. However, inherent defects, structural disorder, and large-scale flexibility are commonly found throughout this family of materials and constitute active research areas.[2] In particular, a growing number of noncrystalline MOFs have been reported, ranging from MOF liquids to MOF gels and including a large variety of glassy states and amorphous solids produced by different physical or chemical routes.[3] While retaining the intrinsic advantages of crystals and powders, these states possess distinct physical and chemical properties (isotropy, high transparency, mechanical robustness, etc.) and allow for greater ease of processing, making them suitable for various industrial applications, ranging from gas separation to water treatment and including reversible long-term harmful substance storage.[4,5]

However, the determination of the framework structure of these amorphous MOFs at the microscopic scale is experimentally difficult, with diffraction experiments only providing indirect structural information. In order to work around or alleviate this challenge, an array of computational methods coexist to model these disordered materials, with different scopes, scales, and computational costs.[6] One possible strategy consists in simulating the phase transition from a crystalline MOF to the amorphous state using molecular dynamics (MD) to in silico mimic the experimental formation routes. In prior work in our group, ab initio MD has successfully been used to model the melting of crystalline MOFs into liquids[7−9] and generate configurations of melt-quenched glasses.[10] However, this approach has a very significant computational cost which limits its use to small systems and short timescales. Classical MD simulations, routinely used for crystalline MOFs, do not readily provide a computationally efficient alternative as they are unable to simulate bond breaking or reformation, two processes inherent to the formation of most amorphous MOFs.[11]

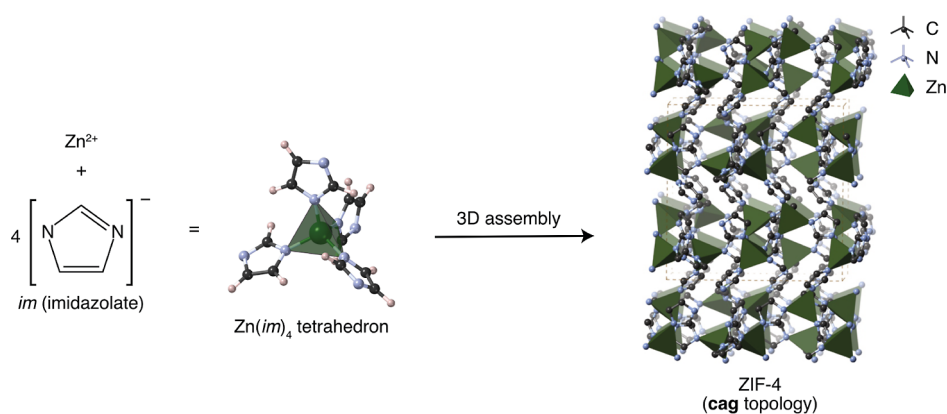Reactive force fields have been proposed as a trade-off between chemical accuracy and computation cost. These
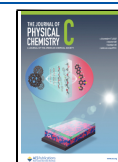
**Figure 1.** Representation of the assembly of ZIF-4 as a three-dimensional network of $Zn(Im)_4$ tetrahedra. Reprinted with permission from ref 6. Copyright 2022 American Chemical Society.

empirical force fields possess connection-dependent terms that enable the simulation of bond breaking and reformation.[12] Starting with the work of Yang et al.,[13] several studies relied on reactive force fields to generate models of zeolitic imidazolate framework (ZIF) glasses by melt quenching and computed various mechanical[14,15] and thermal[16] properties, accessible with the larger spatial and timescales this approach can reach. However, we note that in the existing literature, the generated models have not been subjected to direct and in-depth comparison with those obtained by alternative approaches.[6]

In this work, we probe the accuracy and reliability of modeling the formation and structure of amorphous ZIFs using the ReaxFF reactive force field. We first reproduce the melt-quenching procedure used in prior works,[13] highlighting several difficulties and suggesting adaptations to the scheme. We then detail the structure of the resulting glasses and compare it to ab initio data,[10] contrasting their properties and commenting on some peculiarities of the glasses obtained with reactive force fields. Our system throughout this study will be ZIF-4, which is built from $Zn^{2+}$ metal nodes and imidazolate (Im) organic linkers. As illustrated in Figure 1, its building units are organized in the crystalline state as $Zn(Im)_4$ tetrahedra linked by Zn−N coordinative bonds. The first discovered amorphous MOF[17] has since been the subject of numerous studies, both experimental and numerical, thus providing a prototypical amorphous ZIF system.

## COMPUTATIONAL METHODS

**Reactive Force Field and MD Parameterization.** We employed the reactive force field for ZIF materials introduced by Yang et al.[13] Consisting in a parameterization of ReaxFF,[12] a flavor of reactive force fields, it has since then been used in several computational studies of ZIF glasses. Initially developed for the study of Zn−Im complexes in aqueous solution at room temperature, and validated with ab initio data for these systems,[18] this reactive force field was then transferred and used to generate amorphous ZIFs.

All simulations were performed using large-scale atomic/molecular massively parallel simulator (LAMMPS).[19,20] A time step of 0.25 fs was used in the MD runs and, the temperature (and pressure when applicable) was controlled using a Nosé−Hoover thermostat (and barostat). Unless otherwise specified, temperature and pressure damping parameters are fixed at 100 and 1000 fs, respectively. At every stage, several values were tested to check the relevance of this range. By default,

constant-pressure $(N, P, T)$ simulations are performed using an isotropic cell, using the LAMMPS keyword iso. To reduce finite size effects, a $(2 \times 2 \times 2)$ supercell of ZIF-4 with 2176 atoms was simulated, with periodic boundary conditions as in Yang et al.[13] We checked that it does not significantly affect the properties of the generated glasses (see Figure S1).

Representative input files for the MD simulations are available online in our data repository at https://github.com/fxcoudert/citable-data.

**Trajectory Analysis.** Unless explicitly stated in the legend, properties were averaged over an $(N, V, T)$ trajectory of 1 ns for ReaxFF systems and 60 ps for ab initio simulations. For ReaxFF simulations, frames were taken every 125 fs for the radial distribution function (RDF), bond angle distribution, and coordination number, every 250 fs for the mean square displacement (MSD), every 10 ps for ring statistics, and every 25 ps for pore statistics. For ab initio simulations, these intervals were, respectively, 0.5 fs, 5 fs, 0.5 ps, and 0.5 ps.

**Potential of Mean Force.** The potential of mean force (PMF)[21] is computed from partial RDFs $g(r)$ through the relation $F(r) = -k_B T(\ln g(r) - \ln g_{max})$, where $g_{max}$ is the maximum of $g(r)$ over $r$ which is used to enforce a reference of $F(r) = 0$ for the lowest free energy minimum.[7] The angular PMF is computed from the angle distribution $P(\theta)$ through the analog relation $F_{ang}(\theta) = -k_B T(\ln P(\theta) - \ln P_{max})$.[22] The PMF curves can highlight areas of the coordinate space where the RDF and bond angle distributions have very small, but nonzero, values.

**Coordination Number and Angle Distribution.** Zn−N coordination numbers and N−Zn−N angle distributions are computed by taking a cutoff radius of 2.5 Å, a value determined based on the Zn−N PMF, and validated in previous ab initio studies.[7,8,10] We checked that the outcome of the calculations for ReaxFF systems is not strongly dependent on the exact value chosen in the 2.5−2.7 Å range.

**Lindemann Ratio.** The Lindemann ratio $\Delta$ is computed from partial RDFs $g(r)$, following the same procedure as the previous ab initio studies[7,8,10]

$$\Delta = \frac{fwhm}{d_0}$$

where fwhm is the full-width at half-maximum of the first peak in $g(r)$ (estimated by a Gaussian fit) and $d_0$ corresponds to the mean interatomic distance, calculated as the distance $r$ corresponding to the maximum of the first peak of $g(r)$.

**Pore Statistics.** The total pore volume was computed on individual frames using Zeo++[23−25] as the sum of accessible and nonaccessible volumes. We used a helium probe of radius 1.2 Å and the high accuracy (-ha) option.

**Identification of Building Units.** The identification of building units—metal nodes (Zn) and organic ligands (imidazolate, denoted Im)—in a glass is more challenging than for crystals, especially at high temperatures due to larger fluctuations in the bond angles and lengths, as well as the presence of defects in the coordination. We developed aMOF, a Python library, to reduce the atomic structure into a structure made of Zn and Im. It is detailed in the Supporting Information, and the code is available online at https://github.com/coudertlab/amof, where the version used for this work corresponds to the tag jphyschem.

**Ring Statistics.** Ring statistics were computed using the R.I.N.G.S. code[26] on the Zn−Im periodic graph obtained after the identification of the building units. The vertices of this graph are the Zn atoms and Im linkers, and its edges are the Zn−Im bonds.

The definition of rings used in this work corresponds to the definition of "primitive rings," first introduced by Marians[27] and used in the R.I.N.G.S. code.[26] Several names referring to the same mathematical object can be found in the literature, and this definition is equivalent to that of "shortest path ring" by Franzblau,[28] of "minimal ring" by Guttman,[29] of "irreducible ring" by Wooten,[30] and of "rings" by Goetzke and Klein.[31]

A path between vertices $y$ and $z$ of length $k$ is a chain of $k$ edges joining $y$ to $z$, in which at most two edges share any vertex. A cycle is a closed path; that is, it returns to its starting point. A ring is a cycle of a graph which contains the shortest path for each pair of vertices. A detailed outline of this terminology can be found in Franzblau[28] or any of the other references above.

We used a maximum search depth of 32, safely above the largest rings of the ZIF-4 crystal (16), and we checked that for the studied ZIF-4 glasses, the choice of the maximum search depth did not significantly affect the analysis and conclusions drawn.

## RESULTS AND DISCUSSION

**Producing Glass Models with In Silico Melt-Quenching.** In order to generate atomistic models of ZIF glasses, we have decided to follow the melt-quenching route, reproducing the increase in temperature with MD simulations to produce a liquid ZIF,[7] followed by a quench back to room temperature to produce a glass. This general procedure, mimicking the experimental reality (albeit at length and timescales that are much shorter), has long been used to model the structure of multiple glass-forming materials such as chalcogenide compounds or silicates.[32−34] It has previously been used in simulations of ZIFs, both with a reactive force field[13] and with ab initio MD.[10]

In this work, we followed the same general melt-quenching procedure with small adaptations. Using the ReaxFF force field, an initial crystalline structure was prepared and heated up to 300 K, allowing us to measure the properties of the ZIF in its crystalline phase. Then, the system was melted by heating it to a maximal temperature (well above the melting point). The produced liquid was then quenched to room temperature, transitioning into the glass state. Finally, the system was equilibrated, and its structural and dynamic properties were

calculated. Both the melt quenching and the equilibration were performed in the constant-pressure ($N$, $P$, $T$) ensemble to be able to capture changes in density during the formation. The four steps of this procedure are presented in Figure 2.
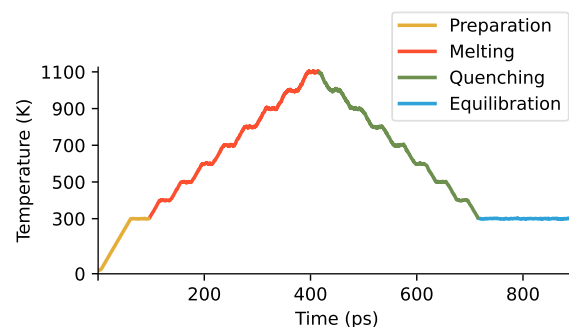


**Figure 2.** Temperature as a function of time during the glass formation procedure with ReaxFF, consisting of preparation (orange), melting (red), quenching (green), and equilibration (blue). Plateaus are present to collect statistics during melt quenching. For clarity, only the start of the equilibration is shown, and a moving average over 250 fs is used. An enlarged plot of the preparation is presented in Figure S2.

**Preparation of the Crystal.** While it may seem trivial to equilibrate the crystal structure at room temperature, we want to detail this here because we have found that it is a crucial step. This is true in particular when we want to simulate with ReaxFF structures that originate from different levels of theory or come from experiments, therefore with different structural characteristics—for which features of the original model should be retained. We do this by imposing constraints on the energy, temperature, and volume of the system and successively releasing them.

After initial energy minimization, the system is relaxed at a very low temperature, using a constant-volume ($N$, $V$, $T$) ensemble at 20 K for 5 ps with a temperature damping parameter of 10 fs (necessary to avoid having too large forces and a high temperature in the initial dynamics, as can be seen otherwise by checking the thermodynamic properties of this initial low-temperature relaxation).

The system then needs to be brought to 300 K, staying in the ($N$, $V$, $T$) ensemble to decouple temperature and pressure equilibration. We tried various heating rates from 2.5 to 116 K/ps, the value chosen in Yang et al.[13] We found that rates above 10 K/ps lead to the breaking of Zn−N bonds, with the coordination number dropping from the expected value of 4. This undesirable and unphysical decoordination has consequences on the final structural properties of the obtained crystals, illustrated with the potentials of mean force (PMF) shown in Figure S3. Due to the reactive nature of this force field, it is advised to carefully check that no bond breaking happens in the crystalline state.[7] We therefore chose a safe value of 5 K/ps for the heating rate of the preparation.

Finally, once 300 K is reached, we switched to the constant-pressure ($N$, $P$, $T$) ensemble at $P = 0$ Pa, with a pressure damping parameter of 1000 fs and using an isotropic cell. After a short equilibration period of 30 ps, we found that this constant-pressure simulation led to an increase in density from 1.21 to 1.3. We checked that using a longer equilibration period of 500 ps does not change the properties of the resulting glass. We tried using a flexible cell (LAMMPS

keyword tri) and found that it led to a dramatic increase in density (up to 1.6), shown in Figure S4. The goal being system stabilization, it led us to keep the isotropic constraint on the cell shape. This tendency to densify will be discussed in the final section. Several pressure damping parameters in the range of 250 to 4000 fs were tested, leading to no significant change in the final density.

**Melt Quenching.** The equilibrated ZIF-4 crystal is then heated above its melting temperature before being cooled down, with constant heating and cooling rates. While these rates are necessarily several orders of magnitude higher than in any achievable experiment, due to the small timescales tractable by MD simulations,[34] they should be low enough to simulate a quasi-static process. Yang et al. opted for 96 K/ps[13] and the subsequent ReaxFF works used the lower value of 24 K/ps.[14−16] A cooling rate of 50 K/ps was chosen for the ab initio work to ensure the tractability of the simulation but was then seen as a limitation of the work.[10] Using the computational effectiveness of reactive force fields, we opted here for heating and cooling rates of 2.5 K/ps.

To monitor structural properties as a function of temperature during melt quenching, such as the RDF plotted in Figure S5, we opted for subsequent steps of a temperature ramp-up of 100 K at 5 K/ps and plateaus of 20 ps. As shown in Figure 2, this succession of steps is equivalent to effective heating and cooling rates of 2.5 K/ps. We checked that the presence or absence of plateaus (with the same effective rate) has no influence on the final glasses' properties, as expected for a quasi-static simulation. We also checked, and demonstrate in Figure S6, that in the 1.25−5 K/ps range, the precise value does not significantly change the outcome of the simulation. We note here again that melt-quenching simulations were performed in the $(N, P, T)$ ensemble with an isotropic cell, as the use of a flexible cell led to an undesirable fast density increase in the first tens of picoseconds, which affects the final properties of the melt-quenched glass.

**Choice of the Melting Temperature.** The choice of the maximal temperature, necessarily above the melting temperature, is a trade-off between the need to gather statistics on relatively rare events during the relatively short times explored in MD,[7] and the necessity to preserve the physical consistency of the model. A value of 1500 K was chosen for both the previous ab initio[10] and ReaxFF[13−16] works. While ab initio MD simulations of the liquid ZIF have been performed up to 2000 K while preserving the integrity of the imidazolate linkers,[7] no published work has investigated the temperature stability of ReaxFF simulations of the ZIF liquid.

During melting with a 2.5 K/ps heating rate, we report that when the maximal temperature exceeds 1300 K for more than a few tens of picoseconds, the system vaporizes (as shown in Figure S7). This effect is kinetically kinetically hidden when using the faster heating rates of 24−96 K/ps that do not provide sufficient time for the system to equilibrate, explaining why it was not observed in the previous ReaxFF works.[13−16] It suggests a tendency of this reactive force field to be overly favorable to zinc−Im bond-breaking events, which is exacerbated at such high temperatures.

Additionally, we observe that when the system temperature is above 1100 K for a sufficiently long time, a number of imidazolates are no longer properly treated, for example, with an opening of the imidazolate ring as reported in Figure S8. This unphysical treatment of the organic linkers, which should be stable at the melting temperature,[7] is more visible for lower

heating/cooling rates as they lengthen the time spent at high temperatures and increase the proportion of open rings. It could nonetheless be observed when we reproduced the high melting rate of 96 K/ps and maximal temperature of 1500 K of Yang et al.[13]

Changing the maximal temperature to 1100 K to avoid these undesired effects has significant implications for the computed structural properties. As shown in Table 1, the decoordination

**Table 1. Coordination Numbers for Nitrogen Atoms around the Zinc Cation of ZIF-4 Glasses for Different Maximal Temperatures, Compared to Previous ReaxFF[13] and Ab Initio[10] Works**

|  | this work | | Yang et al.[13] | ab initio[10] |
|---|---|---|---|---|
| maximal temperature | 1100 K | 1300 K | 1500 K | 1500 K |
| Zn−N average coordination | 3.85 | 3.59 | 3.56 | 3.93 |

of the Zn atoms compared to the crystal is now in better agreement with ab initio data[10] than in previous ReaxFF works. Similarly, the Zn−N PMF shown in Figure 3 indicates a higher
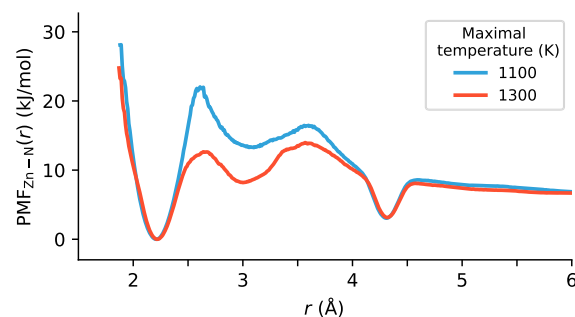


**Figure 3.** PMF for Zn−N of melt-quenched ReaxFF glass produced with two different maximal temperatures.

free-energy barrier to bond breaking, closer to the ab initio structure (see next section). This suggests that these imidazolate breaking events are frequent enough to statistically change the structural properties, and thus, we recommend verifying that they do not appear during melt-quenching.

Having opted for a lower maximal temperature of 1100 K, it is crucial to check that this value is still high enough for the crystal to melt. This is first evidenced by computing the MSD over time, shown in Figure 4a for Zn. At temperatures above 1000 K, we identify a diffusive behavior for the system, as expected for a liquid. In addition, similarly to previous ab initio works,[7,8] we computed the generalized Lindemann ratio[35] from the width of the first peak in the Zn−N partial RDF. A solid is usually considered to be melting when the value of this ratio, which quantifies the liquid nature of the system, is between 10 and 15%. Although less precise than the MSD, this estimate, shown in Figure 4b, provides further evidence that the system is in a liquid state at 1100 K.

**Equilibration.** Finally, after the melt-quenching procedure, the glass model obtained was then equilibrated for 20 ps in the same $(N, P, T)$ ensemble as during melt quenching, the duration of one constant temperature plateau. The simulation was then further run for production during 1 ns in the $(N, V, T)$ ensemble to gather statistics of structural and dynamical properties of the glass. We checked that up to 10 ns of further equilibration in the $(N, P, T)$ ensemble, even with a flexible
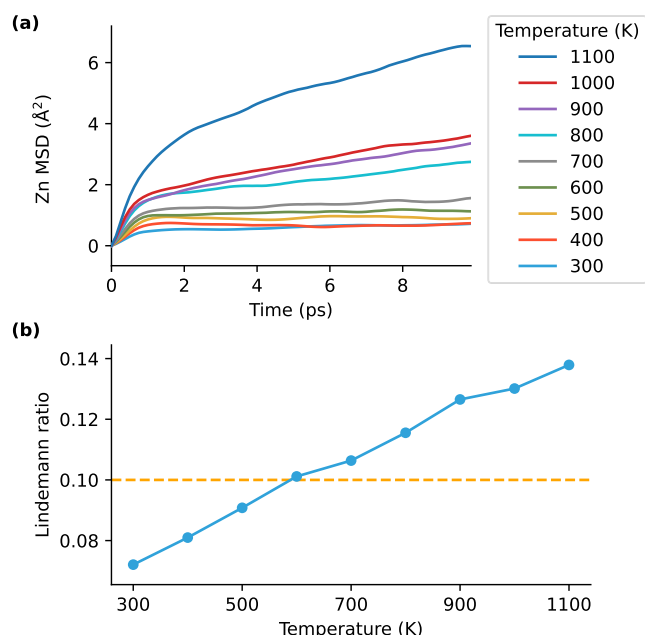
**Figure 4.** Evidence of melting during the ReaxFF glass generation. (a) MSD as a function of time for Zn for temperatures ranging from 300 to 1100 K. (b) Generalized Lindemann ratio, as a function of temperature, calculated for Zn−N interatomic distances. The orange horizontal line represents a "critical ratio" at 10%.

cell, does not perceptibly change the measured properties of the glass.

**Properties of the Glass Models.** In order to quantitatively evaluate the validity of the ReaxFF melt-quenched glass model, we have compared its structural characteristics with that of glass models generated at a higher level of theory, namely, the ab initio models of the work by Gaillac et al.,[10] obtained with density functional theory-based MDs. Such ab initio simulations allow for a full description of the electronic state of the system at the quantum chemical level and still represent the most reliable atomistic description of ZIF-4 glasses published to date in the literature.[6]

Due to the significant computational cost of ab initio MD, a faster melt-quenching procedure was used: only the quenching from a 1500 K liquid was simulated, with a faster cooling rate (50 K/ps), on a smaller system (unit cell) and with a shorter equilibration (~100 ps). To limit the impact of finite size effects, 10 quenched glasses were generated and their properties were averaged. Due to the difficulty of performing $(N, P, T)$ ab initio simulations of such flexible frameworks,[36] all ab initio simulations were performed in the $(N, V, T)$ ensemble. Although the influence of the density on the crystal and liquid properties was evaluated in previous work,[7] the inability to capture changes in density remains an important limitation of this ab initio methodology.[6] The ab initio simulation of a crystal at 300 K reported here comes from the same work.[7,10]

**Local Order: Interatomic Distances and Bond Angles.** We first investigated the difference in the local order between ReaxFF and ab initio glasses by examining the metal−ligand bonds (Zn−N), central to the $Zn(Im)_4$ tetrahedral structure represented in Figure 1. For the two models, we plot and compare the partial RDFs $g(r)$ for the Zn−N atom pairs in Figure 5 and for Zn−Zn pairs in Figure S9. As outlined in Table 2, we find a shift in Zn−N atomic distances of 0.2 Å
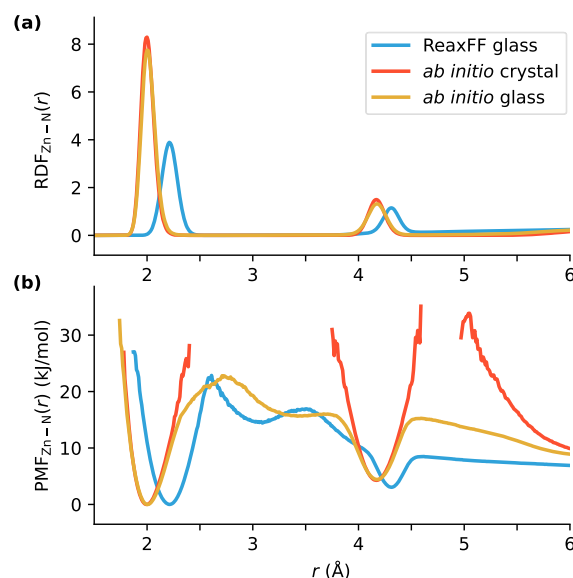


**Figure 5.** (a) RDFs and (b) PMF for the Zn−N atom pairs of the ReaxFF glass (blue), ab initio glass (orange), and ab initio crystal (red).

**Table 2. Interatomic Distances (Zn−N and Zn−Zn) of the ReaxFF ZIF-4 Glass Compared to Ab Initio and Experimental Values**[a]

| | Zn−N (Å) | Zn−Zn (Å) |
|---|---|---|
| ReaxFF glass | 2.21 | 6.35 |
| ab initio glass | 2.00 | 5.97 |
| ab initio crystal | 2.00 | 5.97 |
| experimental crystal | 1.97 (XRD[37]), 1.98 (NMR[38]) | 5.87 (XRD[37]) |
| experimental glass | 1.99 (RMC[7]) | 5.95 (RMC[7]) |

[a]Experimental data is obtained from X-ray diffraction studies[37] and NMR[38] for the crystal, and a RMC refinement of neutron and X-ray scattering data of a melt-quenched glass.[7]

between ReaxFF and both the ab initio and experimental values. To contrast the differences of the partial RDF in the region between the first two peaks, we also present it in the form of a PMF. From the resultant free-energy profiles, we observe similar values for the free-energy barriers ($\simeq$23 kJ/mol), although with different shapes. The wider well and narrower barrier for the ReaxFF glass suggest a tendency of ReaxFF to allow Zn−N bonds to break more easily.

Yet, the most stringent distinctive feature of the ReaxFF glass compared to its ab initio counterpart lies in the N−Zn−N bond angle distribution $P(\theta)$, shown in Figure 6. From the $Zn(Im)_4$ tetrahedral structure, we expect a unimodal distribution of around 109° for the crystal. Experimentally measured by nuclear magnetic resonance (NMR),[38] this feature is well reproduced for the ab initio crystal. Due to the undercoordination of a small fraction of the $Zn^{2+}$ nodes in the glasses, a small deviation is expected and observed for the ab initio glass, with a wider distribution and tail at higher angle values. However, the ReaxFF glass distribution is very different, with a broad distribution of angles on the 70−170° spectrum. This distribution is unphysical and does not reproduce the known tetrahedral chemistry of the system, suggesting ill-adjusted angle constraints in the force field. The angular PMF shown in Figure 6 further evidences the tendency of this force field to have the ReaxFF glass deform too easily.
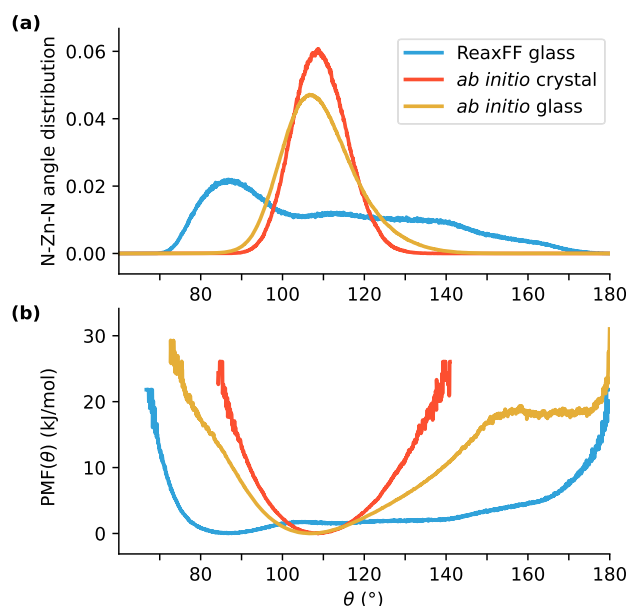
**Figure 6.** (a) Distribution and (b) PMF of the N−Zn−N angle for the ReaxFF glass (blue), ab initio glass (orange), and ab initio crystal (red).

that a larger value is expected for the glass. Although we could expect the difference in crystallographic densities between the glass and crystal to be much smaller, the complex diffusion behavior of helium into the ZIF-4 pores makes pycnometric densities measurements difficult to interpret. As an alternative to pycnometry, a recent work determined the crystallographic density of the ZIF-4 glass from $CO_2$ physisorption studies.[40] Estimated to be 1.38 g cm$^{-3}$, this value hints that ReaxFF overestimates the glass density.

Additionally, we computed the porosity of the glasses (see Figure S10) and found a total porous volume of 4.6 cm$^3$ kg$^{-1}$ for the ReaxFF glass, down from 54 cm$^3$ kg$^{-1}$ of the crystal (computed for ab initio). As the porosity is greatly impacted by the density of a system, direct comparison to the ab initio glass (68 cm$^3$ kg$^{-1}$) is limited but does suggest that the ReaxFF glass porosity is one order of magnitude too low. All these but complete loss of porosity also contradict the experimental measurements of the porosity of a ZIF-4 glass made by positron annihilation lifetime spectroscopy[42] and further confirm that the density of the ReaxFF glass is excessively large.

**Topological Properties of the Coordination Network.** Finally, we investigated the differences in the medium-range order of the glasses, highlighted by their contrasting structure factors shown in Figure S11, by examining the coordination network built from the alternating Zn−Im units. We first calculated the average Zn−N coordination numbers and found a lower coordination of 3.85 for the ReaxFF glass compared to 3.93 for the ab initio glass, confirming the ReaxFF tendency to underconstrain Zn−N bonds.

In order to characterize the topology at a larger scale, known to be key to the properties of these framework materials,[43] we computed Zn−Im ring statistics. This analysis is routinely used to characterize amorphous systems such as $SiO_2$[26] and first applied to amorphous MOFs for the ab initio glasses,[10] determines the number and size of rings present in the ZIF network. Ring sizes are computed by counting the number of different units (Zn and Im) in each ring; always even, they are equal to twice the T-based ring sizes usually reported for zeolitic nets.[44] These distributions of ring sizes, reported in Figure 7, show that both glasses have topologies that deviate from the crystal perfectly defined 8, 12, and 16 rings. However, the two glass models display very different topologies, with the ReaxFF glass having a higher proportion of larger rings than the ab initio glass. It demonstrates that it is less ordered at the medium range, a result arising from the too-weak constraints on the Zn−Im interactions.
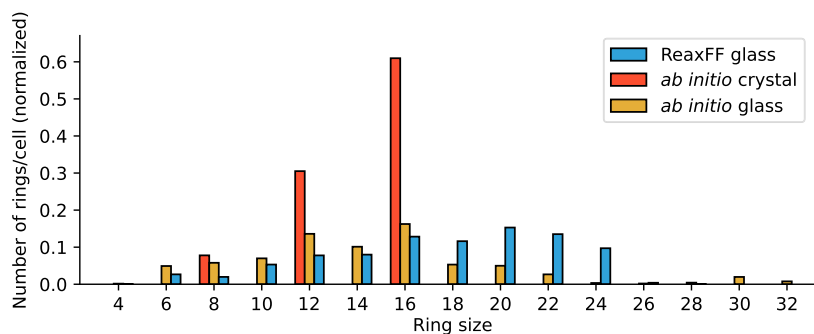
Despite the importance of the N−Zn−N angle for the framework properties, key to the features of ZIFs, we found that statistical distributions of bond angles have never been published in the existing literature on ReaxFF simulations of these materials: Yang et al. showed the results of a single frame,[13] while a later work by To et al. only looked at the average bond angle.[15] We recommend computing and reporting this distribution in the same way as it is routinely done for the development of classical force fields.[39]

**Bulk Properties: Density and Porosity.** By allowing exaggerated deformation of the framework, the underconstrained Zn−Im interactions described above impact the bulk properties of the ReaxFF glass. We report from our simulations a density of 1.68 g cm$^{-3}$, significantly larger than the crystal density of 1.21 g cm$^{-3}$. Comparison with the ab initio glass is not possible as they were generated using a constant-volume $(N, V, T)$ ensemble, which does not capture changes in density. Direct experimental comparison of these densities computed from the atomic structure is limited: they correspond to crystallographic densities, while almost all densities measurements performed for glasses utilized pycnometry.[40] Nevertheless, pycnometric densities of 1.63 g cm$^{-3}$ for the glass and 1.50 g cm$^{-3}$ for the crystal[41] indicate



**Figure 7.** Distributions of the size of zinc−Im alternate rings for the ReaxFF glass (blue), ab initio glass (orange), and ab initio crystal (red).

**Challenges in Using ReaxFF.** In addition to generating a glass model markedly different from its ab initio counterpart, we identified several challenges when using the ReaxFF force field for ZIFs. We highlight them here as they should be kept in mind and may be applicable to other molecular simulations of MOF glasses.

**(N, P, T) Ensemble and Densification.** MDs simulations in the constant-pressure (N, P, T) ensemble are remarkably insightful, notably for the study of mechanical and thermal properties.[11,45] Yet, previous work has shown that they are particularly challenging to apply to soft porous materials due to the sensitive response of these frameworks to small external stimuli,[6] in particular for ab initio calculations.[36] While every published work on ZIFs with ReaxFF used (N, P, T) ensembles, no systematic validation has been published to this day.

In order to evaluate the robustness of such constant-pressure simulations, we equilibrated at T = 300 K and P = 0 Pa several ZIF-4 systems: the crystal, three ab initio glasses models from ref 10, and a glass obtained by reverse Monte Carlo (RMC) modeling.[7,46] These systems, thoroughly presented in the Supporting Information, went through the preparation process detailed in the first section. They were then equilibrated between 5 and 20 ns in the (N, P, T) ensemble with a flexible cell. More general than an isotropic cell, a flexible cell enables the computation of multiple mechanical properties using the strain−fluctuation method,[47] already applied to ZIFs using classical force fields.[11] As reported in Table 3, we see that the

**Table 3. Densities after Preparation and Equilibration in ReaxFF for the ZIF-4 Crystal and Three ZIF-4 Glasses, Compared to Their Initial Densities**

|  | initial density (g cm$^{-3}$) | density after equilibration (g cm$^{-3}$) |
|---|---|---|
| crystal | 1.21 | 1.61 |
| ReaxFF glass |  | 1.68 |
| RMC glass | 1.58 | 1.56 |
| ab initio glass | 1.21 | 1.57 |

density of every equilibrated system is in the range of 1.5−1.7 g cm$^{-3}$, regardless of their initial density. We conclude that the large density observed for the ReaxFF glass may not be due to its specific structure but is rather a symptom of ReaxFF's tendency to densify systems.

We have found that using an isotropic cell for the crystal and ab initio glasses reduces the magnitude of the densification, respectively, by 0.25 g cm$^{-3}$ (see Figure S4) and 0.14 g cm$^{-3}$ (see Figure S12). This difference, which should a priori not be observed for the crystal as the cell shape is not supposed to vary much, highlights once again that this ReaxFF force field is very sensitive and does not fare well when we reduce the number of constraints on the system. Nevertheless, we recommend using an isotropic cell if one has no interest in the fluctuations of the cell, as it provides a behavior closer to the physical reality.

Another option to avoid this undesired densification may consist in staying in the constant-volume (N, V, T) ensemble, similar to what was done in the ab initio works.[7,10] For example, pressure equilibration can be achieved by successive slow deformation of the cell until zero pressure is reached. When we performed this procedure in the case of the ZIF-4 crystal, it leads to a density of 1.26 g cm$^{-3}$, not far from the

experimental crystal density. However, although this approach could fix the troublesome densification, we end up losing all the benefits of the (N, P, T) ensemble that every ReaxFF work published so far was interested in.

**Description of the Crystal.** Surprisingly, we found that the ReaxFF parameterization for Zn-based ZIFs has not been systematically validated on any crystalline structure in the existing literature. Therefore, we report here the properties of a ZIF-4 crystal prepared as described in the first section. The goal is to differentiate the intrinsic properties of the ReaxFF glass from the numerical artifacts linked to the use of this force field. Due to the ReaxFF tendency to densify the crystal, we investigated various equilibration procedures using either (N, V, T) or (N, P, T) ensembles, which are detailed in the Supporting Information.

These various strategies led to ReaxFF crystals of different densities, reported in Table S1, which ineluctably lead to different porosities (see Figure S13). Under (N, V, T) simulations, we systematically found no change in the connectivity (see Table S1) or topology of the crystal (see Figure S14). However, this does not hold true for the (N, P, T) schemes for which we observe a small deviation, evidencing that an (N, P, T) equilibration at 300 K causes undesired bond breaking, even when enforcing an isotropic cell.

An investigation of the local order with the RDF and PMF (see Figure S15) evidences a similar shift in interatomic distances compared to ab initio data to what was observed for the glass. Additionally, we observe a significant lowering of the free-energy barrier in the PMF between the first two minima compared to the ab initio data, even for the crystal systems that never went through an (N, P, T) ensemble. This tendency to systematically underconstrain the Zn−N interaction is further evidenced by the unphysical bond angle distribution shown in Figure 8. Unphysical angles are also observed on two other ZIF crystals—ZIF-8 and SALEM-2—evidencing that this issue is not linked to the choice of ZIF-4 as a prototypical system (see Figure S16). We conclude that the unphysical description of the zinc−imidazolate coordination in the ReaxFF force field
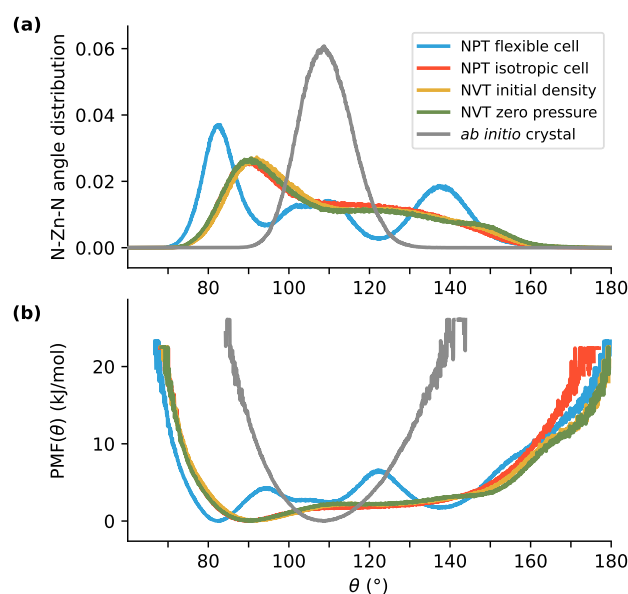


**Figure 8.** (a) Distribution and (b) PMF of the N−Zn−N angle for the ReaxFF crystals with four different equilibrations, compared to the ab initio crystal.

also manifests in the detailed analysis of the structural properties of the crystalline phase, further questioning the validity of this force field.

## CONCLUSIONS AND PERSPECTIVES

In this work, we have extensively studied the use of the ReaxFF reactive force field to generate atomistic models of ZIF glasses. We have demonstrated that the molecular simulations performed so far in the literature are extremely sensitive to the choice of simulation methodology and parameters: thermodynamic ensemble, damping parameters, heating/cooling rate, maximal temperature, and so forth. The physical consistency of the system should always be carefully checked, for example, by drawing inspiration from the procedure presented in this study.

We have also shown that the glass models generated with ReaxFF are markedly different from their ab initio counterparts, with extensive differences in both local environments, medium-range, and bulk properties. We find that this is due in large part to an underconstrained representation of the Zn−N interactions in the ReaxFF model, which do not faithfully reproduce one of the key characteristics of the chemistry of ZIFs, namely, the directional nature of the Zn−N coordination. This issue in the intermolecular potential, in turn, significantly impacts the crystal properties obtained through molecular simulations. Additionally, we have reported and analyzed a tendency of simulations performed in the constant-pressure $(N, P, T)$ ensemble to densify the system.

All these observations suggest that structural properties obtained from the use of the ReaxFF force field for ZIFs should be interpreted with caution and make a strong case for the use of alternative methodologies or the further optimization of the ReaxFF force field. They also call for further methodological development to assess the possibility to explore the mechanical properties of these soft porous materials with ReaxFF. Moreover, we recommend for future developments of ZIF reactive force fields to systematically check their ability to simulate an $(N, P, T)$ equilibration of the crystal at ambient conditions. A good example of such practice is the recent development of a ReaxFF force field for zirconium-based MOFs by the same group, for which the authors reported the density profile for a 1 ns equilibration.[48]

Finally, this work exemplifies the need for a direct and in-depth comparison of the different models of ZIF glasses available by systematically contrasting their properties. It shows that, apart from expensive ab initio calculations, no MDs scheme used to this date in the literature[6] can yield an accurate microscopic representation of the ZIF melt-quenched glasses and suggests the development of multiscale modeling strategies. A possible strategy could consist in the use of classical force fields, more robust and parameterized for specific systems,[39] to analyze glass models (e.g., compute their mechanical properties) formed by other methodologies. Another promising strategy, aiming at the actual generation of MOF glasses using less expensive MD schemes, is the development of machine-learning potentials.[49,50] Built from ab initio data, they enable bond breaking and reformation by design and could constitute a new generation of specific and accurate reactive potentials.

## ASSOCIATED CONTENT

### Ⓢ Supporting Information

The Supporting Information is available free of charge at https://pubs.acs.org/doi/10.1021/acs.jpcc.2c06305.

> System description for the $(N, P, T)$ runs and ReaxFF crystals, identification of the building units, RDFs, PMF, angle distributions, coordination numbers, densities, porous volumes, and ring statistics (PDF)

## AUTHOR INFORMATION

### Corresponding Author

**François-Xavier Coudert** − *Chimie ParisTech, PSL Research University, CNRS, Institut de Recherche de Chimie Paris, 75005 Paris, France;* ⓘ orcid.org/0000-0001-5318-3910; Email: fx.coudert@chimieparistech.psl.eu

### Author

**Nicolas Castel** − *Chimie ParisTech, PSL Research University, CNRS, Institut de Recherche de Chimie Paris, 75005 Paris, France; École des Ponts, 77420 Marne-la-Vallée, France;* ⓘ orcid.org/0000-0002-0572-3940

Complete contact information is available at: https://pubs.acs.org/10.1021/acs.jpcc.2c06305

### Notes

The authors declare no competing financial interest.

## ACKNOWLEDGMENTS

## REFERENCES

(1) Furukawa, H.; Cordova, K. E.; O'Keeffe, M.; Yaghi, O. M. The Chemistry and Applications of Metal-Organic Frameworks. *Science* **2013**, *341*, 1230444.

(2) Bennett, T. D.; Coudert, F.-X.; James, S. L.; Cooper, A. I. The changing state of porous materials. *Nat. Mater.* **2021**, *20*, 1179−1187.

(3) Bennett, T. D.; Horike, S. Liquid, glass and amorphous solid states of coordination polymers and metal−organic frameworks. *Nat. Rev. Mater.* **2018**, *3*, 431−440.

(4) Bennett, T. D.; Cheetham, A. K. Amorphous Metal−Organic Frameworks. *Acc. Chem. Res.* **2014**, *47*, 1555−1562.

(5) Fonseca, J.; Gong, T.; Jiao, L.; Jiang, H.-L. Metal−organic frameworks (MOFs) beyond crystallinity: amorphous MOFs, MOF liquids and MOF glasses. *J. Mater. Chem. A* **2021**, *9*, 10562−10611.

(6) Castel, N.; Coudert, F.-X. Atomistic Models of Amorphous Metal−Organic Frameworks. *J. Phys. Chem. C* **2022**, *126*, 6905−6914.

(7) Gaillac, R.; Pullumbi, P.; Beyer, K. A.; Chapman, K. W.; Keen, D. A.; Bennett, T. D.; Coudert, F.-X. Liquid metal−organic frameworks. *Nat. Mater.* **2017**, *16*, 1149−1154.

(8) Gaillac, R.; Pullumbi, P.; Coudert, F.-X. Melting of Zeolitic Imidazolate Frameworks with Different Topologies: Insight from First-Principles Molecular Dynamics. *J. Phys. Chem. C* **2018**, *122*, 6730−6736.

(9) Widmer, R. N.; Lamapronti, G. I.; Anzellini, S.; Gaillac, R.; Farsang, S.; Zhou, C.; Belenguer, A. M.; Wilson, C. W.; Palmer, H.; Kleppe, A. K.; et al. Pressure promoted low-temperature melting of metal−organic frameworks. *Nat. Mater.* **2019**, *18*, 370−376.

(10) Gaillac, R.; Pullumbi, P.; Bennett, T. D.; Coudert, F.-X. Structure of Metal−Organic Framework Glasses by Ab Initio Molecular Dynamics. *Chem. Mater.* **2020**, *32*, 8004−8011.

(11) Ortiz, A. U.; Boutin, A.; Fuchs, A. H.; Coudert, F.-X. Investigating the Pressure-Induced Amorphization of Zeolitic Imidazolate Framework ZIF-8: Mechanical Instability Due to Shear Mode Softening. *J. Phys. Chem. Lett.* **2013**, *4*, 1861−1865.

(12) Senftle, T. P.; Hong, S.; Islam, M. M.; Kylasa, S. B.; Zheng, Y.; Shin, Y. K.; Junkermeier, C.; Engel-Herbert, R.; Janik, M. J.; Aktulga, H. M.; et al. The ReaxFF reactive force-field: development, applications and future directions. *npj Comput. Mater.* **2016**, *2*, 15011.

(13) Yang, Y.; Shin, Y. K.; Li, S.; Bennett, T. D.; van Duin, A. C. T.; Mauro, J. C. Enabling Computational Design of ZIFs Using ReaxFF. *J. Phys. Chem. B* **2018**, *122*, 9616−9624.

(14) To, T.; Sørensen, S. S.; Stepniewska, M.; Qiao, A.; Jensen, L. R.; Bauchy, M.; Yue, Y.; Smedskjaer, M. M. Fracture toughness of a metal−organic framework glass. *Nat. Commun.* **2020**, *11*, 357.

(15) To, T.; Sørensen, S. S.; Yue, Y.; Smedskjaer, M. M. Bond switching is responsible for nanoductility in zeolitic imidazolate framework glasses. *Dalton Trans.* **2021**, *50*, 6126−6132.

(16) Sørensen, S. S.; Østergaard, M. B.; Stepniewska, M.; Johra, H.; Yue, Y.; Smedskjaer, M. M. Metal−Organic Framework Glasses Possess Higher Thermal Conductivity than Their Crystalline Counterparts. *ACS Appl. Mater. Interfaces* **2020**, *12*, 18893−18903.

(17) Bennett, T. D.; Goodwin, A. L.; Dove, M. T.; Keen, D. A.; Tucker, M. G.; Barney, E. R.; Soper, A. K.; Bithell, E. G.; Tan, J.-C.; Cheetham, A. K. Structure and Properties of an Amorphous Metal-Organic Framework. *Phys. Rev. Lett.* **2010**, *104*, 2272.

(18) Shin, Y. K.; Ashraf, C. M.; van Duin, A. C. T.Development and Applications of the ReaxFF Reactive Force Field for Biological Systems. *Computational Materials, Chemistry, and Biochemistry: From Bold Initiatives to the Last Mile*; Springer International Publishing: Cham, 2021; pp 157−182.

(19) Thompson, A. P.; Aktulga, H. M.; Berger, R.; Bolintineanu, D. S.; Brown, W. M.; Crozier, P. S.; in 't Veld, P. J.; Kohlmeyer, A.; Moore, S. G.; Nguyen, T. D.; et al. LAMMPS - a flexible simulation tool for particle-based materials modeling at the atomic, meso, and continuum scales. *Comput. Phys. Commun.* **2022**, *271*, 108171.

(20) Aktulga, H.; Fogarty, J.; Pandit, S.; Grama, A. Parallel reactive molecular dynamics: Numerical methods and algorithmic techniques. *Parallel Comput.* **2012**, *38*, 245−259.

(21) Chandler, D.*Introduction to Modern Statistical Mechanics*; Oxford University Press, 1987.

(22) Mu, Y.; Kosov, D. S.; Stock, G. Conformational Dynamics of Trialanine in Water. 2. Comparison of AMBER, CHARMM, GROMOS, and OPLS Force Fields to NMR and Infrared Experiments. *J. Phys. Chem. B* **2003**, *107*, 5064−5073.

(23) Willems, T. F.; Rycroft, C. H.; Kazi, M.; Meza, J. C.; Haranczyk, M. Algorithms and tools for high-throughput geometry-based analysis of crystalline porous materials. *Microporous Mesoporous Mater.* **2012**, *149*, 134−141.

(24) Pinheiro, M.; Martin, R. L.; Rycroft, C. H.; Jones, A.; Iglesia, E.; Haranczyk, M. Characterization and comparison of pore landscapes in crystalline porous materials. *J. Mol. Graphics Modell.* **2013**, *44*, 208−219.

(25) Pinheiro, M.; Martin, R. L.; Rycroft, C. H.; Haranczyk, M. High accuracy geometric analysis of crystalline porous materials. *CrystEngComm* **2013**, *15*, 7531.

(26) Le Roux, S.; Jund, P. Ring statistics analysis of topological networks: New approach and application to amorphous GeS₂ and SiO₂ systems. *Comput. Mater. Sci.* **2010**, *49*, 70−83.

(27) Marians, C. S.; Hobbs, L. W. Network properties of crystalline polymorphs of silica. *J. Non-Cryst. Solids* **1990**, *124*, 242−253.

(28) Franzblau, D. S. Computation of ring statistics for network models of solids. *Phys. Rev. B: Condens. Matter Mater. Phys.* **1991**, *44*, 4925−4930.

(29) Guttman, L. Ring structure of the crystalline and amorphous forms of silicon dioxide. *J. Non-Cryst. Solids* **1990**, *116*, 145−147.

(30) Wooten, F. Structure, odd lines and topological entropy of disorder of amorphous silicon. *Acta Crystallogr., Sect. A: Found. Crystallogr.* **2002**, *58*, 346−351.

(31) Goetzke, K.; Klein, H.-J. Properties and efficient algorithmic determination of different classes of rings in finite and infinite polyhedral networks. *J. Non-Cryst. Solids* **1991**, *127*, 215−220.

(32) *Molecular Dynamics Simulations of Disordered Materials*; Massobrio, C., Du, J., Bernasconi, M., Salmon, P. S., Eds.; Springer International Publishing: Cham, 2015.

(33) Benoit, M.; Ispas, S.; Tuckerman, M. E. Structural properties of molten silicates from ab initio molecular-dynamics simulations: Comparison between CaO−Al₂O₃−SiO₂ and SiO₂. *Phys. Rev. B: Condens. Matter Mater. Phys.* **2001**, *64*, 1044.

(34) Li, X.; Song, W.; Yang, K.; Krishnan, N. M. A.; Wang, B.; Smedskjaer, M. M.; Mauro, J. C.; Sant, G.; Balonis, M.; Bauchy, M. Cooling rate effects in sodium silicate glasses: Bridging the gap between molecular dynamics simulations and experiments. *J. Chem. Phys.* **2017**, *147*, 074501.

(35) Chakravarty, C.; Debenedetti, P. G.; Stillinger, F. H. Lindemann measures for the solid-liquid phase transition. *J. Chem. Phys.* **2007**, *126*, 204508.

(36) Haigis, V.; Belkhodja, Y.; Coudert, F.-X.; Vuilleumier, R.; Boutin, A. Challenges in first-principles NPT molecular dynamics of soft porous crystals: A case study on MIL-53(Ga). *J. Chem. Phys.* **2014**, *141*, 064703.

(37) Park, K. S.; Ni, Z.; Côté, A. P.; Choi, J. Y.; Huang, R.; Uribe-Romo, F. J.; Chae, H. K.; O'Keeffe, M.; Yaghi, O. M. Exceptional chemical and thermal stability of zeolitic imidazolate frameworks. *Proc. Natl. Acad. Sci. U.S.A.* **2006**, *103*, 10186−10191.

(38) Madsen, R. S. K.; Qiao, A.; Sen, J.; Hung, I.; Chen, K.; Gan, Z.; Sen, S.; Yue, Y. Ultrahigh-field ⁶⁷Zn NMR reveals short-range disorder in zeolitic imidazolate framework glasses. *Science* **2020**, *367*, 1473−1476.

(39) Dürholt, J. P.; Fraux, G.; Coudert, F.-X.; Schmid, R. Ab Initio Derived Force Fields for Zeolitic Imidazolate Frameworks: MOF-FF for ZIFs. *J. Chem. Theory Comput.* **2019**, *15*, 2420−2432.

(40) Frentzel-Beyme, L.; Kolodzeiski, P.; Weiß, J.-B.; Schneemann, A.; Henke, S.Quantification of gas-accessible microporosity in metal-organic framework glasses. *ChemRxiv***2022** DOI: 10.26434/chemrxiv-2021-lq308-v2.

(41) Bennett, T. D.; Yue, Y.; Li, P.; Qiao, A.; Tao, H.; Greaves, N. G.; Richards, T.; Lam.; Lamponti, G. I.; Redfern, S. A. T.; Blanc, F.; et al. Melt-Quenched Glasses of Metal−Organic Frameworks. *J. Am. Chem. Soc.* **2016**, *138*, 3484−3492.

(42) Thornton, A. W.; Jelfs, K. E.; Konstas, K.; Doherty, C. M.; Hill, A. J.; Cheetham, A. K.; Bennett, T. D. Porosity in metal−organic framework glasses. *Chem. Commun.* **2016**, *52*, 3750−3753.

(43) Widmer, R. N.; Lamponti, G. I.; Chibani, S.; Wilson, C. W.; Anzellini, S.; Farsang, S.; Kleppe, A. K.; Casati, N. P. M.; MacLeod, S. G.; Redfern, S. A. T.; et al. Rich Polymorphism of a Metal−Organic Framework in Pressure−Temperature Space. *J. Am. Chem. Soc.* **2019**, *141*, 9330−9337.

(44) Baerlocher, C.; McCusker, L. B.; Olson, D. H.*Atlas of Zeolite Framework Types*, 6th ed.; Elsevier Science B.V.: Amsterdam, 2007.

(45) du Bourg, L. B.; Ortiz, A. U.; Boutin, A.; Coudert, F.-X. Thermal and mechanical stability of zeolitic imidazolate frameworks polymorphs. *APL Mater.* **2014**, *2*, 124110.

(46) McGreevy, R. L. Reverse Monte Carlo modelling. *J. Phys.: Condens. Matter* **2001**, *13*, R877−R913.

(47) Parrinello, M.; Rahman, A. Strain fluctuations and elastic constants. *J. Chem. Phys.* **1982**, *76*, 2662−2666.

(48) Dwivedi, S.; Kowalik, M.; Rosenbach, N.; Alqarni, D. S.; Shin, Y. K.; Yang, Y.; Mauro, J. C.; Tanksale, A.; Chaffee, A. L.; van Duin, A. C. Atomistic Mechanisms of Thermal Transformation in a Zr-Metal Organic Framework, MIL-140C. *J. Phys. Chem. Lett.* **2020**, *12*, 177−184.

(49) Behler, J. First Principles Neural Network Potentials for Reactive Simulations of Large Molecular and Condensed Systems. *Angew. Chem., Int. Ed.* **2017**, *56*, 12828−12840.

(50) Eckhoff, M.; Behler, J. From Molecular Fragments to the Bulk: Development of a Neural Network Potential for MOF-5. *J. Chem. Theory Comput.* **2019**, *15*, 3793−3809.